LSD flattens the brain's energy landscape: evidence from receptor-informed network control theory

S. Parker Singleton[A]*, Andrea I. Luppi[B,C], Robin L. Carhart-Harris[D], Josephine Cruzat[E,F], Leor Roseman[D], Gustavo Deco[F,G,H,I], Morten L. Kringelbach[J,K,L], Emmanuel A. Stamatakis[B], Amy Kuceyeski[A,M]

[A] Department of Computational Biology, Cornell University, Ithaca, USA

[B] Division of Anesthesia, School of Clinical Medicine, University of Cambridge, Cambridge, United Kingdom

[C] Department of Clinical Neurosciences, University of Cambridge, Cambridge, United Kingdom

[D] Center for Psychedelic Research, Department of Brain Science, Imperial College London, London, United Kingdom

[E] Latin American Brain Health Institute (BrainLat), Universidad Adolfo Ibanez, Santiago, Chile

[F] Center for Brain and Cognition, Computational Neuroscience Group, Department of Information and Communication Technologies, Universitat Pompeu Fabra, Roc Boronat 138, Barcelona, Spain

[G] Institució Catalana de la Recerca i Estudis Avançats (ICREA), Passeig Lluís Companys 23, Barcelona, Spain

[H] Department of Neuropsychology, Max Planck Institute for Human Cognitive and Brain Sciences, Leipzig, Germany

[I] School of Psychological Sciences, Monash University, Melbourne, Clayton, Australia

[J] Department of Psychiatry, University of Oxford, Oxford, United Kingdom

[K] Center of Music in the Brain (MIB), Clinical Medicine, Aarhus University, Denmark

[L] Centre for Eudaimonia and Human Flourishing, University of Oxford

[M] Department of Radiology, Weill Cornell Medicine, New York, USA

*Corresponding author
Email address: sps253@cornell.edu (S. Parker Singleton)

Abstract:

Psychedelics like lysergic acid diethylamide (LSD) offer a powerful window into the function of the human brain and mind, by temporarily altering subjective experience through their neurochemical effects. The RElaxed Beliefs Under Psychedelics (REBUS) model postulates that 5-HT2a receptor agonism allows the brain to explore its dynamic landscape more readily, as suggested by more diverse (entropic) brain activity. Formally, this effect is theorized to correspond to a reduction in the energy required to transition between different brain-states, i.e. a "flattening of the energy landscape." However, this hypothesis remains thus far untested. Here, we leverage network control theory to map the brain's energy landscape, by quantifying the energy required to transition between recurrent brain states. In accordance with the REBUS model, we show that LSD reduces the energy required for brain-state transitions, and, furthermore, that this reduction in energy correlates with more frequent state transitions and increased entropy of brain-state dynamics. Through network control analysis that incorporates the spatial distribution of 5-HT2a receptors, we demonstrate the specific role of this receptor in flattening the brain's energy landscape. Also, in accordance with REBUS, we show that the occupancy of bottom-up states is increased by LSD. In addition to validating fundamental predictions of the REBUS model of psychedelic action, this work highlights the potential of receptor-informed network control theory to provide mechanistic insights into pharmacological modulation of brain dynamics.

Significance Statement:

We present a multi-modal framework for quantifying the effects of a psychedelic drug (LSD) on brain dynamics by combining functional magnetic resonance imaging (fMRI), diffusion MRI (dMRI), positron emission tomography (PET) and network control theory. Our findings provide support for a fundamental theory of the mechanism of action of psychedelics by showing that LSD flattens the brain's energy landscape, allowing for more facile and frequent state transitions and more temporally diverse brain activity. We also demonstrate that the spatial distribution of serotonin 2a receptors - the main target of LSD - is key for generating these effects. This approach could be used to understand how drugs act on different receptors in the brain to influence brain function.

Introduction:

Serotonergic psychedelics like lysergic acid diethylamide (LSD) induce a profound but temporary alteration of perception and subjective experience[1]. Combined with non-invasive neuroimaging such as functional MRI, these drugs offer a unique window into the function of the human mind and brain, making it possible to relate mental phenomena to their neural underpinnings.

The insight provided by neuroimaging studies of psychedelics over the last decade has culminated in a recent model of psychedelic action, known as RElaxed Beliefs Under Psychedelics (REBUS). This model integrates previous accounts of psychedelic action with the view of the brain as a prediction engine, whereby perception and belief are shaped by both prior knowledge and incoming information[2–4]. The REBUS model postulates that psychedelics alter cognitive functioning by serotonergic action at 5-HT2a receptors in higher-order cortical regions. Dysregulation of these regions' activity results in a weaker effect of prior beliefs and expectations in shaping the interpretation of bottom-up information, ultimately allowing the brain to explore its dynamic landscape more readily - as suggested by more diverse (entropic) brain activity. In accordance with the REBUS model, recent work has also provided indirect evidence of relaxed priors as the decreased coupling of structural and functional connectivity networks under LSD - thereby facilitating access to physiological states less constrained by anatomical connections[5]. Formally, relaxed priors are theorized to correspond to a reduction in the energy required to transition between different brain-states, i.e., a "flattening of the energy landscape". However, this hypothesis remains thus far untested.

One avenue to understand how psychedelics influence brain activity is through neurobiologically informed whole-brain computational models. Through these types of approaches, recent work has shown that the effects of serotonergic psychedelics on the dynamics of human brain activity are critically dependent on their action at 5HT2a receptors. Whole-brain neural-mass models have implicated the 5-HT2a receptor distribution across the cortex in shaping brain dynamics under the effects of LSD and psilocybin[6,7], as well as demonstrating a role for 5-HT2a receptor agonism in increasing the temporal diversity (entropy) of brain activity in a way that is consistent with empirical observations[8].

An alternative computational approach to modelling brain dynamics is network control theory, which focuses on quantifying and controlling how a dynamical system moves through its state space. It is well-known that even at rest the brain is not static, but rather it dynamically alternates between a number of recurrent states[9–16]. Such recurrent brain-states may be relevant for cognition[17–20] and even consciousness[21–27], and have been shown to undergo prominent reorganization during the psychedelic state induced by LSD[5,6] and psilocybin[7,28]. Crucially, network control theory approaches enable mapping of the brain's energy landscape by quantifying the energy required to transition between these recurrent states (Figure 1a,b). Recent work utilized these tools to demonstrate that although the resting human brain has a spontaneous tendency to prefer certain brain-state transitions over others, cognitive demands can overcome this tendency in a way that is associated with age and cognitive performance. This work demonstrates that network control theory approaches can reveal neurobiologically and cognitively relevant brain activity dynamics[29,30].

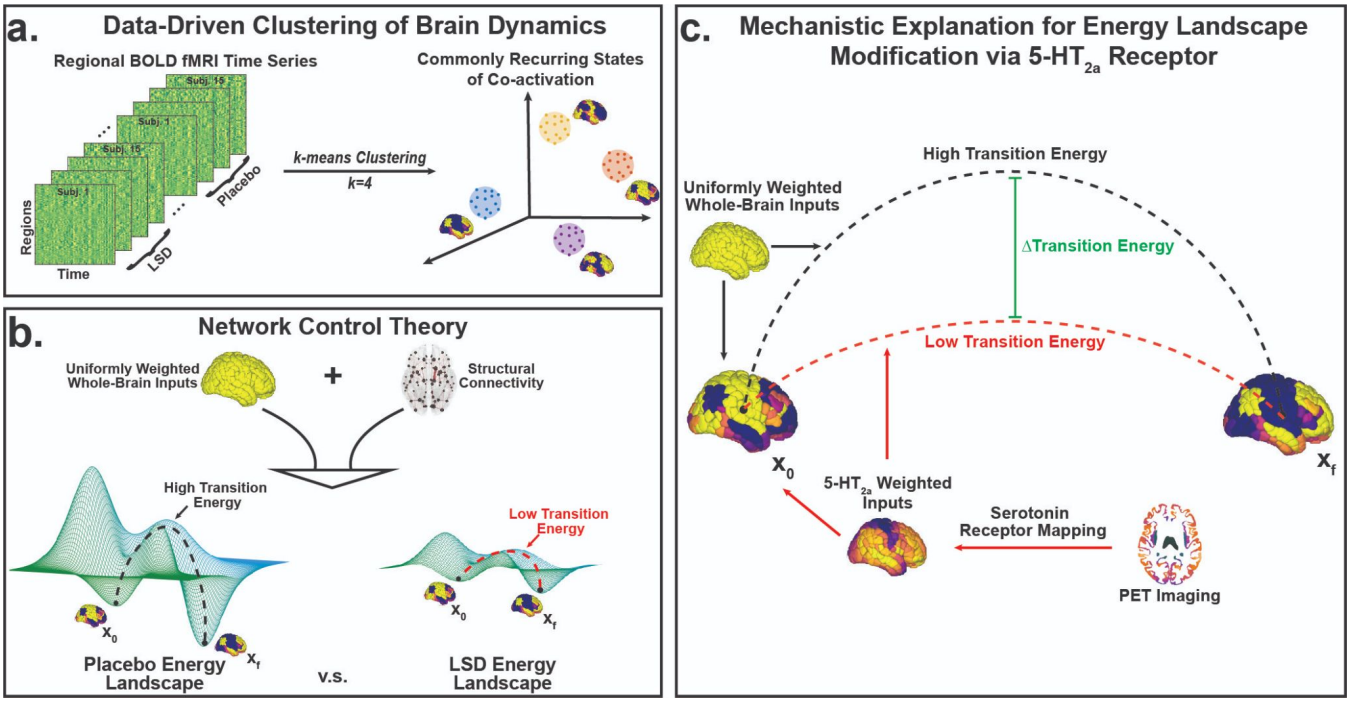

Figure 1. Mapping the energy landscape of the human brain with network control theory. (a) We concatenated all fMRI time series together (all subjects, all conditions) and employed the *k*-means clustering algorithm to identify common activation patterns, or states. **(b)** Using network control theory and a representative structural connectome[31], we calculated the minimum energy required to transition between states (or maintain the same state) using each individual's brain-states derived from the LSD and placebo conditions separately. Our calculations reveal an energy landscape that is flattened by LSD. **(c)** Weighting the energy calculations of the placebo brain-states with inputs from PET-derived receptor density maps of the serotonin 2a receptor also resulted in a flattened energy landscape, providing a mechanistic explanation for LSD's flattening effect.

Here, we leverage recent advances in network control theory to probe a leading model for the action of psychedelics on the brain: we combine functional MRI data from 15 healthy volunteers under the effects of LSD or placebo, with structural (white-matter) connectivity networks obtained from diffusion MRI (dMRI), and receptor density maps from positron emission tomography (PET). In accordance with the REBUS model, we hypothesized that the energy required to transition between brain states would decrease under LSD compared to placebo. Further, we tested the mechanistic hypothesis that LSD's action at 5-HT2a receptors is responsible for this reduction in transition energy by demonstrating that the specific spatial pattern of 5-HT2a receptor expression flattens the energy landscape more than any other receptor distribution tested (Figure 1c).

Results:

Data-driven clustering of brain activity patterns reveals recurrent states of opposing network activation

We investigated functional MRI data acquired from 15 volunteers over two sessions, either under the influence of the psychedelic LSD or a placebo[32], to address the central tenet of the leading REBUS

model[2] of psychedelic action on the human brain and mind. Namely, does LSD induce a "flattening" of the brain's energy landscape, and, furthermore, is this effect a result of 5HT2A receptor agonism?

Our first step was to identify recurrent states of brain activity. One commonly used approach to identifying recurrent brain-states is through the k-means clustering algorithm[6,7,29,33], whereby brain activation patterns from each individuals' scans are grouped into a pre-specified number of clusters *k*. Here, data-driven clustering of regional activity patterns identified *k*=4 stable clusters that achieved optimal division of the data (see *Materials and Methods: Extraction of Brain-states* for choice of *k*). The four clusters can be divided into two meta-states (Meta-State 1 and Meta-State 2, Figure 2), each composed of two sub-states that represent opposing activation patterns (SOM+/- and FPN+/-, Figure 2). Dichotomy of the brain's dynamic states has previously been observed[29,34] and is consistent with hierarchical organization[35,36].

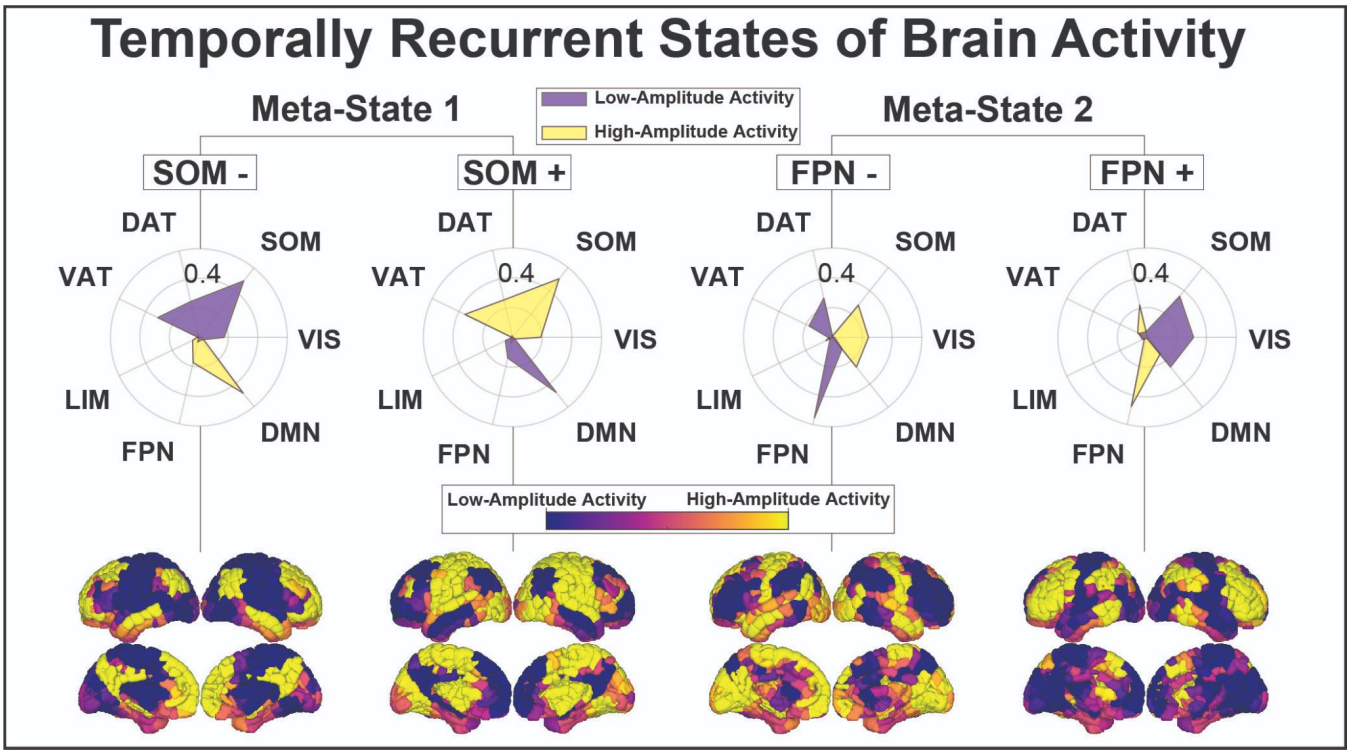

Figure 2. Recurrent states of brain activity. Group-average recurrent brain-states are represented by the mean activation pattern across all subjects and conditions for each of the 4 clusters (brain representations at the bottom of the figure). For each brain-state, we separately calculated the cosine similarity of its high-amplitude (supra-mean) activity and low-amplitude (sub-mean) activity to a priori resting-state networks[37] (RSNs); resulting similarity measures are represented via radial plots[29]. Meta-State 1 (MS-1) is characterized by the contraposition of the somatomotor and ventral attention/salience networks with the default-mode network, whereas the Meta-State 2 (MS-2) is characterized by the contraposition of the default-mode, somatomotor and visual networks with the frontoparietal network. We therefore label them as SOM+/- (for MS-1) and FPN+/- (for MS-2) to indicate the main RSN that has the highest amount of overlap (defined as maximum cosine-similarity) with the brain-state and its amplitude. The dichotomy of these states can be observed visually in the radial plots and on the rendered brain volumes, and is confirmed via their negative, significant Pearson correlation (SI Figure 2, ii).

LSD modulates brain dynamics by increasing occupancy in bottom-up, somatomotor-dominated brain-states

To identify the effects of LSD on brain-state dynamics, each subject's fMRI data were characterised in terms of the four identified brain-states. From each subject's temporal sequence of brain-states (Figure 3a) we obtained a systematic characterization of the temporal dynamics of the 4 states, namely, their (i) fractional occupancies, or the probability of occurrence of each state (Figure 3b, i), (ii) dwell times, or the mean duration that a given state was maintained, in seconds (Figure 3b, ii), (iii) appearance rates, or how often each state appeared per minute (Figure 3b, iii), and (iv) transition probabilities, or the probability of switching from each state to every other state (Figure 4a, i).

We found that for both LSD and placebo conditions, the brain most frequently occupies the SOM+/- state (higher fractional occupancy) whose constituent sub-states are also visited for the longest periods of time (highest dwell times) (Figure 3b). LSD modifies the fractional occupancy of these states by decreasing the dwell times of FPN+/- and further increasing dwell times of the already dominant SOM+/- (Figure 3b). No differences in appearance rate for the 4 sub-states was found when comparing the LSD and placebo conditions.

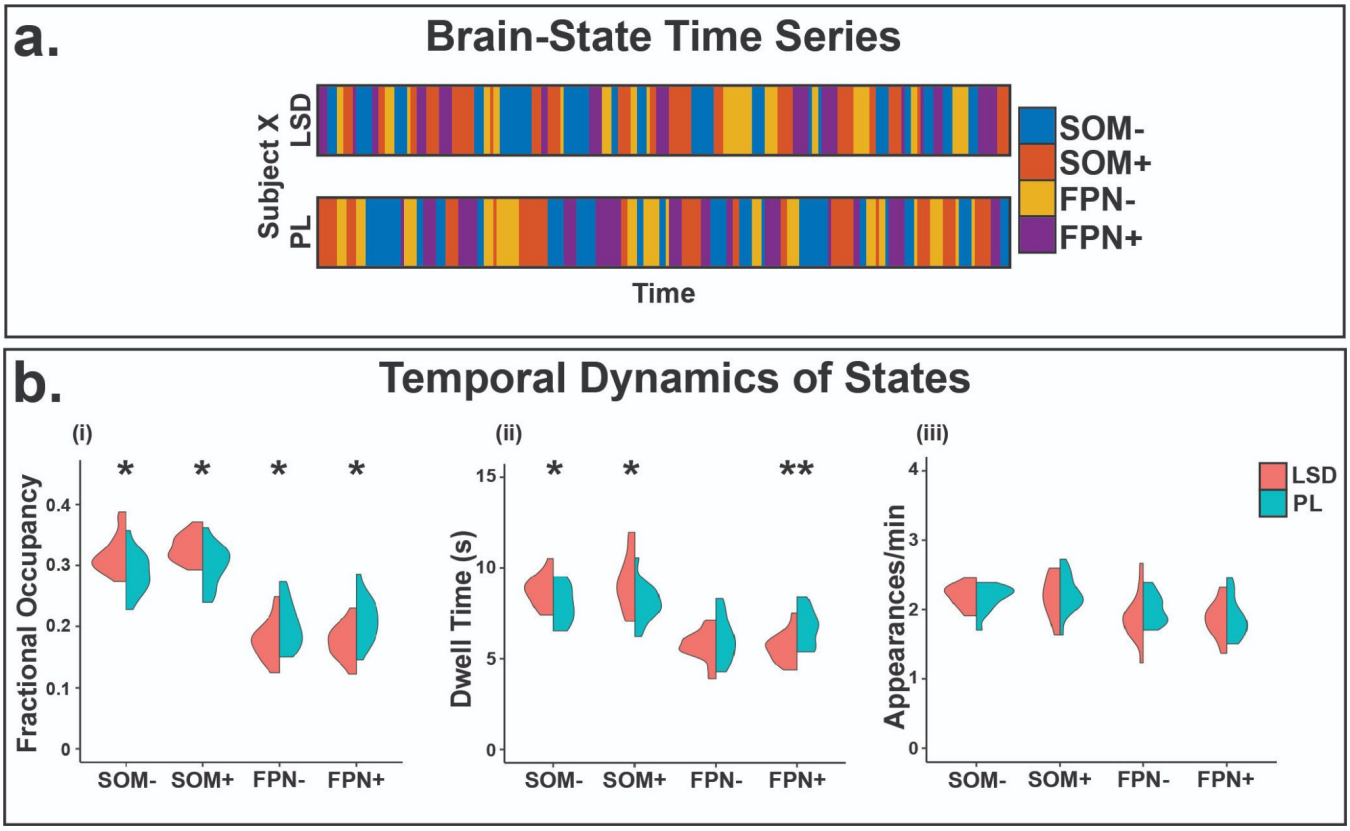

Figure 3: Temporal brain dynamics shift under LSD. (a) *k*-means clustering of the BOLD time series resulted in a brain-state time series for each of the individuals' two scans[29]. **(b)** We then calculated each brain-states' (i) fractional occupancy, (ii) average dwell time, and (iii)average number of appearances per minute for each individual and condition. *significant before multiple comparisons correction, ** significant after multiple comparisons correction.

Empirical transition probabilities were calculated independently for each individual and each condition (Figure 4a, i). Since the SOM+/- meta-states are characterized by prominent engagement of the bottom-up somatomotor and ventral attention/salience networks, we hypothesised that under LSD the brain should transition more frequently to these states, since the REBUS model predicts a shift in favour of bottom-up processing under the effects of psychedelics. Our analysis of transition probabilities supported this hypothesis (Figure 4a, i, diagonal). The increased persistence of states (SOM-) dominated by somatomotor/salience (bottom-up) activity and correspondingly, the decreased persistence of states (FPN+) dominated by frontoparietal (top-down) activity seen under LSD fits with a flattening of the functional hierarchy proposed by REBUS[2,38].

Network control theory reveals LSD-induced flattening of the brain's energy landscape.
However, we sought to provide a more direct test of the REBUS model's hypothesis about LSD's decreased energy requirement to transition between different states. To this end, we turned to network control theory[29,30,39–41], which offers a framework to quantify the ease of state transitions in a dynamical system. Specifically, we calculated the transition energy (TE), which is the minimum amount of energy that would need to be injected into a network (here, the structural connectome[31]) to induce transitions between the possible states of its functional dynamics (note that the transition energy from a given state to itself is the energy required to remain in that state, sometimes referred to as "persistence energy"). For each subject and condition, we calculated the energy needed to transition between each pair of brain-states. Comparing the two conditions, we found that LSD lowered the TE (Figure 4a, ii) between all possible combinations of initial and final brain-states.

Importantly, network control theory requires a specification of a set of "control points" where energy is injected into the system to induce the desired transition. For the previous analysis, we chose uniform inputs over all brain regions. However, one can also ask whether this effect may be driven by a specific set of regions[29]. This is relevant because the changes in brain function under investigation in the present study arise from the administration of LSD. The serotonin 2a (5-HT2a) receptor is well established as the site responsible for the subjective[13–17] and neural[5–7] effects of LSD and other classic serotonergic psychedelics, and this receptor is not uniformly distributed across the brain[47]. Therefore, we sought to determine if the specific regional distribution of 5HT2a receptors in the brain could correspond to especially suitable control points for inducing a reduction in transition energy.

To test this hypothesis, we utilized a high resolution *in vivo* atlas of the serotonin receptor 5HT2a derived from PET imaging to extract biologically relevant weights for our model[30,47]. First, we recalculated the energy matrices for the placebo condition, this time weighting the energy injected into every region in proportion to its amount of 5-HT2a expression. In every possible transition, we observed that the 5-HT2a-weighted inputs provided lower TE than the uniform inputs (Figure 4a, iii).

However, it could be argued that giving additional control to some regions will result in a lower control energy, regardless of the choice of regions. To demonstrate that our results are specific to 5-HT2a receptors' spatial distribution across brain regions, we compared the TEs obtained from the true

5-HT2a distribution, versus 10,000 permutations obtained by randomly reshuffling the spatial positions of the same weights - thereby preserving the set of weights but not the regions they correspond to. The true distribution of 5-HT2a resulted in significantly lower energies (Figure 4a, iv), demonstrating the critical role of the specific regional distribution of 5HT2a receptors for inducing low-energy state transitions such as those empirically observed under the effects of LSD.

In a final demonstration of the specific importance of the 5-HT2a receptor, we investigated the shift in TEs provided by three additional serotonin receptors (5-HT1a, 5-HT1b, 5-HT4) and the serotonin transporter, 5-HTT, all obtained from the same high-resolution PET atlas[35]. We compared the overall mean of the energy matrix for each individual's 2a-weighted calculations versus all others and found that 5-HT2a was the most effective at lowering the overall energy to transition between empirically defined brain-states (Figure 4b). This is especially noteworthy because serotonin 2a receptor agonism plays a prominent role in how LSD and other classic psychedelics influence neural activity[5–7] and subjective experience[13–17]. Together, these results demonstrate that the 5-HT2a receptor is neurobiologically and spatially well-suited for energy landscape flattening - a key tenet of psychedelic action according to the REBUS model.

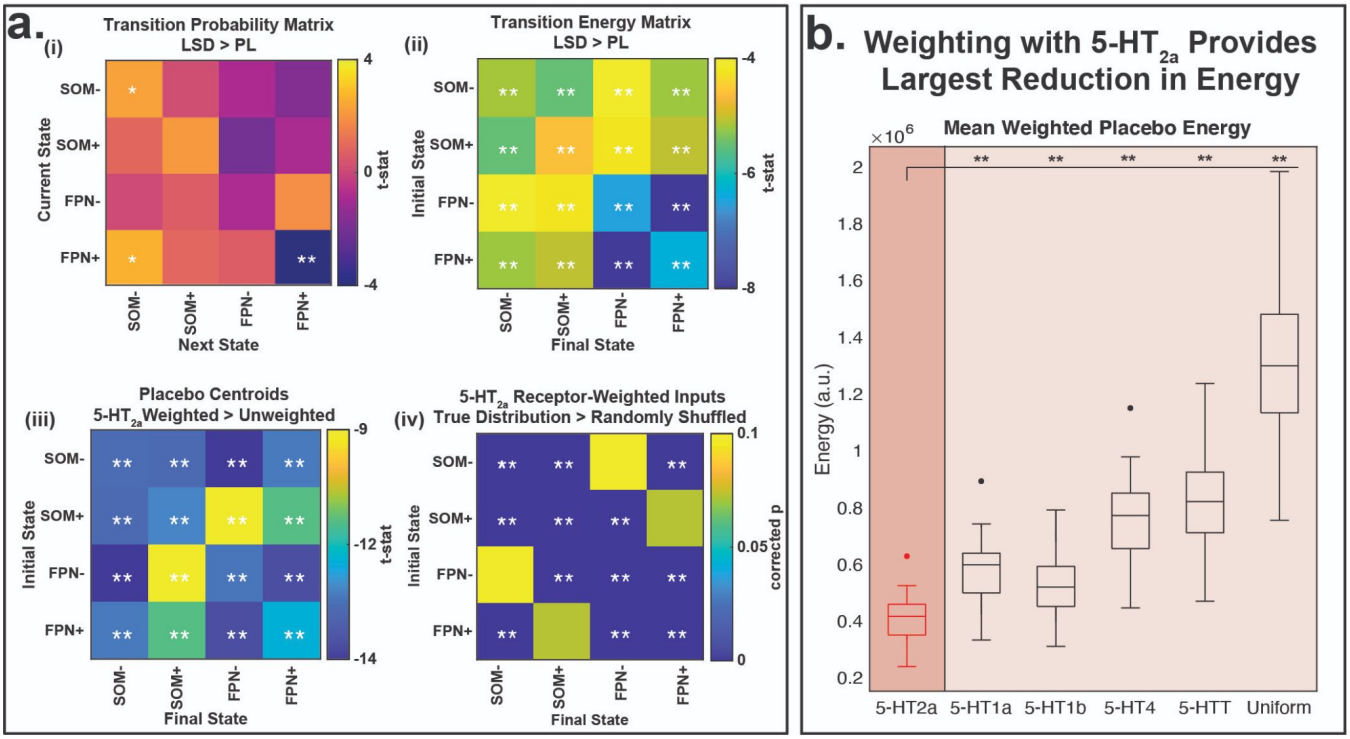

Figure 4: The energy needed to transition between brain states is reduced by LSD and the spatial distribution of 5-HT2a receptor maps. (a) Each of the entries in the four matrices represent the significance and direction of the difference between LSD and placebo for each pair of states. **(a, i)** Comparison of the empirically observed transition probabilities between states, derived from the brain-state time series, e.g. Figure 3a. **(a, ii)** Comparison of the transition energies calculated from placebo brain-states versus those calculated from LSD brain-states using uniformly-weighted whole-brain inputs. LSD brain-states had significantly lower energy required for every transition. **(a, iii)** Weighting with the 5-HT2a receptor density map[47] results in significantly lower energies for the placebo brain-states compared to uniformly-weighted inputs. **(c, iv)** To probe the spatial specificity of part (iii), we repeated the calculations using 10,000 random receptor maps, created by permuting the original 5-HT2a

receptor map. We found that the true 5-HT2a receptor map had significantly lower energy required for nearly every transition compared to the shuffled receptor maps. **(b)** Additionally, we weighted our model with expression maps of other serotonin receptors (5-HT1a, 5-HT1b, and 5-HT4), and the serotonin transporter (5-HTT), and found that 5-HT2a resulted in significantly lower transition energy (averaged across all pairs of states) than all others. (*See SI for choice of the time-span T over which the transition energy was computed*). *significant before multiple comparisons correction, ** significant after multiple comparisons correction.

Increased flattening of the energy landscape is associated with more entropic brain dynamics

Crucially, the results demonstrating the specific role of 5HT2a receptors in flattening the energy landscape were based exclusively on calculations using placebo data. Therefore, we next sought to test how the average TE reduction by LSD (Figure 4a, ii) may affect empirical transition energies and corresponding brain dynamics. Specifically, we show that, across the 15 individuals, the relative change in energy induced by LSD was significantly correlated with the empirically observed changes in state dwell times (Figure 5, i) and appearance rates (Figure 5, ii), $p<0.05$, uncorrected.

Our results show that the more LSD lowered the average transition energy of a given subject, the more the empirically observed dwell times decreased and the more the empirically observed appearance rates increased. The latter is particularly interesting, as there were no group-level differences in appearance rates of individual states between the two conditions. Both findings are consistent with our hypothesis of a flattened energy landscape, where lower barriers between brain-states results in increased frequency of state transitions and shorter state dwell times.

Ratings of the drug's subjective effects were also obtained from each individual (*see SI for details*) and we hypothesized that transition energy reduction by LSD would also predict a more intense subjective experience. We did not find any significant correlations between energy flattening and subjective ratings; extending the present modelling framework to subjective measures may be a fruitful avenue for future research.

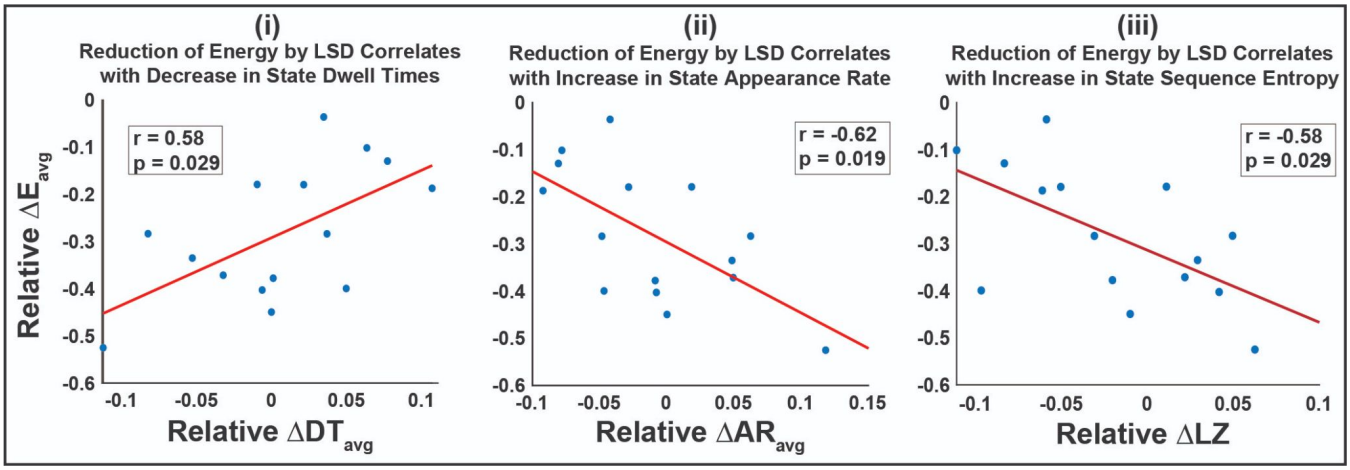

Figure 5: Larger reduction of average transition energy by LSD correlates with more dynamic brain activity across individuals. Significant Pearson correlations exist between an individual's amount of energy reduction by LSD and the relative change in state (i) dwell times, (ii) appearance rates, and (iii) entropy of the brain-state time series. Relative difference was calculated as (LSD - PL)/(LSD + PL). Partial correlations were

calculated while controlling for an individual's head-motion (mean framewise displacement). (uncorrected p-values).

Lastly, we asked whether energy reduction induced by LSD would correlate with more complex (entropic) brain-state time series. This experiment aimed to test the theoretical link between a flatter energy landscape and more entropic brain activity postulated by REBUS[2]. One could imagine a scenario where shorter dwell times and larger appearance rates results in a sequence that is highly predictable (i.e. [1 2 1 2 1 2]). We wanted to test the hypothesis that the true scenario would be the opposite - namely, that a flatter energy landscape would in fact correspond to an increase in the diversity of brain dynamics. Numerous studies have linked changes in the entropy of neuroimaging signals to the psychedelic state[48–52] and the ability for these compounds to increase neural entropy via 5-HT2a agonism is thought to be a key process in the breakdown of the functional hierarchy of the brain and a central component of REBUS[2,3,38]. To test this hypothesis, we used Lempel-Ziv compressibility to compute the entropy rate of the temporal sequence of brain meta-states (SOM and FPN). Supporting our hypothesis, we found that the more a subject's energy landscape was flattened, the more entropic their brain-state time series became (Figure 5, iii). This result directly and quantitatively links the energy of the landscape with empirical changes in entropy rate for the first time and serves as a validation of REBUS' central hypothesis.

Discussion:

Here, we combined fMRI, PET and diffusion MRI with network control theory to test a central tenet of the REBUS model of psychedelic action: namely, that serotonergic psychedelics like LSD induce a "flattening" of the energy landscape in the human brain. A flatter energy landscape corresponds to lower barriers to transition between different states of brain activity. This is theorized to correspond to a flattening of the functional hierarchy as well, i.e. a relaxation of the weighting that high-level priors exert on inputs from lower-level (sensory) regions - thought to be a pivotal component of psychedelics' therapeutic mechanism of action as well as characteristic subjective effects of ego dissolution and visual/auditory distortions[2]. The present results support four central claims of the REBUS model of psychedelic action: (a) more engagement of bottom-up activity, here quantified in terms of increased occurrence of states dominated by SOM and VAT/salience networks, which primarily deal with bottom-up information-processing, (b) a flattening of the brain's energy landscape, indicated by lower energy being required to transition between brain states, and (c) a correlation between flattening of the energy landscape (reduced energy required for state transitions) and more diverse (entropic) sequences of brain activity. Combining fMRI with diffusion MRI and PET information, we were further able to provide computational evidence that (d) the serotonin 2a receptor is especially well-positioned to bring about this flattening of the energy landscape, over and above other 5HT receptors - once again in accordance with theoretical predictions of the REBUS model.

Compared with placebo, subjects in the LSD condition spent a larger fraction of time occupying states characterized by the contraposition of the DMN with bottom-up sensorimotor and salience networks, and less time in states dominated by the contraposition between DMN and top-down fronto-parietal control network (Figure 3b). Since our analysis was carried out on resting-state data, it is not surprising

that the DMN was prominent across all four brain-states[53–56]. However, our results indicating a change in the relative prevalence of FPN-dominated vs SOM-dominated states are in line with the prediction of the REBUS model of increased bottom-up activity under the effects of psychedelics. Additionally, our quantification of the brain's energy landscape through network control theory revealed that LSD lowers the transition energy between all states (Figure 4a, ii).

Given the well-known involvement of 5-HT2a receptors with the neurobiological and subjective effects of LSD, we next sought to determine if the spatial distribution of 5-HT2a receptors across the human cortex could provide a mechanistic explanation for our results. Weighting the model in proportion to the empirical regional density of 5-HT2a receptors obtained from *in vivo* PET imaging[35], we found that the resulting transition energies were greatly reduced, mirroring those of the LSD condition (Figure 4a, iii). Further, to demonstrate the importance of this receptor's spatial distribution, we randomly shuffled the 5-HT2a distribution and found that the original map consistently resulted in lower energies than the shuffled maps (Figure 4a, iv). The calculations were also repeated with other subsets of the 5-HT receptor class, and 5-HT2a was the most effective at reducing energy (Figure 4b), consistent with the known specificity of LSD for this receptor.

The Entropic Brain Hypothesis (EBH)[3,48] proposes that increased neural entropy brought forth by psychedelics is reflected in the subjective experience as an increase in the richness of conscious content - viewing the brain and mind as two sides of the same coin[57]. We found that at an individual subject level, increased LSD-induced transition energy reductions correlated with more dynamic brain activity (Figure 5, i,ii), thereby relating the theoretical interpretation of transition energy with its role in the empirical de-stabilization of brain-state dynamics. Remarkably, we also found that the entropy rate of an individual's sequence of meta-states increased in proportion to the LSD-induced energy reduction (Figure 5, iii), thereby relating the energy landscape of the brain to its entropy. This is especially noteworthy as it provides empirical evidence linking the EBH with the free-energy principle[4] - the two theories that sit at the foundation of REBUS.

More broadly, these results demonstrate that the combination of network control theory and specific information about neurobiology (here exemplified by receptor distributions from PET) can offer powerful insights about brain function and how pharmacology may modulate it - opening the avenue for analogous studies on the effects of pharmacological interventions in clinical populations (e.g. depression, schizophrenia)[30]. While other recent computational approaches have successfully modeled the effects of serotonergic compounds on dynamic brain states[6,7] and the entropy of spontaneous neural activity[8], the present approach is the first to do both while also quantitatively evaluating the energy landscape of the psychedelic state - thereby enabling us to provide empirical support for key theoretical predictions of the REBUS model.

Limitations and Future Work:

Although small sample size is common in neuroimaging studies of psychedelics and other states of altered consciousness due to the inherent difficulties of collecting such data, future replications with larger samples would be appropriate. We also acknowledge that this specific dataset has been studied

extensively before[5,6,8,32,38,52,58–61] and replications in different datasets will be warranted to ensure the generalizability of these results.

It is also important to note that different notions of energy can be employed in neuroscience: the term "energy" used here is a proxy for the variational free-energy of the REBUS model. It should not be confused with metabolic energy of ATP molecules, nor with the energy quantified through connectome harmonic decomposition, which has also been investigated in the context of this same dataset[58,61] and other states of altered consciousness[59]. As employed here, "energy" is to be interpreted as the magnitude of the input that needs to be injected into the system (the brain's structural connectome) in order to obtain the desired state transition.

Additionally, we had hypothesized that the transition energy modifications by LSD would correlate with our participants' subjective experience as captured by intra-scanner visual analog scale ratings, and the 11-factor states of consciousness (ASC) questionnaire[62,63] taken at the end of the day. There may be numerous factors that limit our ability to model these effects. For instance, both subjective experience ratings and the relative energy landscape (baseline or LSD) may be impacted by each individual's prior psychedelic use, individual differences in pharmacological dose response, as well as their own unique structural connectome and 5-HT2a receptor distribution. Indeed, the structural connectome and the PET data used in our analysis were representative examples obtained from population averages, rather than unique data derived from each individual in our study. Although these measures are thought to be less variable across individuals than brain activity dynamics, future work could explore how individual differences in the structural connectome or receptor maps influence the energy landscape - and possibly subjective experiences.

Finally, our approach is based on network control theory, which differs from other recent computational investigations using e.g. whole-brain simulation through dynamic mean-field modelling of brain activity[6–8,23]. These latter approaches employ a neurobiologically realistic model of brain activity based on mean-field reduction of spiking neurons into excitatory and inhibitory populations, and have been used to account for non-linear effects of 5HT2a neuromodulation induced by LSD and other psychedelics. In contrast, network control theory relies on a simpler linear model, which we employed due to its ability to address REBUS's specific prediction about the brain's energy landscape. Additionally, recent evidence suggests that most of the fMRI signal may be treated as linear[64,65]. Combining both approaches to capitalize on the strengths of each will be a fruitful avenue for future work.

Conclusion:

We introduced a framework for receptor-informed network control theory to understand how the serotonergic psychedelic LSD influences human brain function. Combining fMRI, diffusion MRI, PET and network control theory, we presented evidence supporting the hypothesis that LSD flattens the brain's energy landscape and, furthermore, provided a mechanistic explanation for this observed energy reduction by demonstrating that the empirical spatial distribution of 5-HT2a receptor expression is particularly well-suited to flatten the brain activity landscape. This work highlights the potential of receptor-informed network control theory to allow insights into pharmacological modulation of brain function and, importantly, provides evidence to support the REBUS hypothesis of LSD effects.

Materials and Methods:

Data Collection and Processing

Data acquisition is described in detail previously[32]. In brief, twenty healthy volunteers underwent two MRI scanning sessions at least 14 days apart. On one day, participants were given placebo (10 mL saline), and on the other day they received LSD (75 µg in 10 mL saline), infused over two minutes, 115 minutes before resting-state scanning. Post-infusion, subjects had a brief acclamation period in a mock fMRI scanner. On each scanning day, three 7:20 minute eyes-closed resting-state scans were acquired. The first and third scan had no stimulation, while the second scan involved listening to music; this scan was not used in this analysis as we were interested in dynamics in the absence of external stimulation. BOLD fMRI was acquired at 3T with TR/TE = 2000/35ms, FoV = 220mm, 64 × 64 acquisition matrix, parallel acceleration factor = 2, 90 flip angle. Thirty- five oblique axial slices were acquired in an interleaved fashion, each 3.4mm thick with zero slice gap (3.4mm isotropic voxels). One subject was excluded due to anxiety, and 4 due to excessive head motion (> 15% of volumes with mean frame-wise displacement > 0.5), leaving 15 subjects (four women; mean age, 30.5 ± 8.0) for analysis. Data pre-processing utilized AFNI, Freesurfer, FSL and in-house code[32]. Steps included 1) removal of first three volumes; 2) de-spiking; 3) slice time correction; 4) motion correction; 5) brain extraction; 6) rigid body registration to anatomical scans; 7) non-linear registration to 2mm MNI space; 8) scrubbing; 9) spatial smoothing; 10) band-pass filtering (0.01 to 0.08 Hz); 11) de-trending; 12) regression out of 6 motion-related and 3 anatomical-related nuisance regressors. Lastly, time series for 462 gray matter regions[66] were extracted (Lasuanne scale 4, sans brain-stem).

Structural Connectivity Network Construction

Since diffusion MRI was not acquired as part of the LSD study, the structural connectome used for network control theory analysis was identical to the one used in prior work[5]. Namely, we relied on diffusion data from the Human Connectome Project (HCP, http://www.humanconnectome.org/), specifically from 1021 subjects in the 1200-subject release[67]. A population-average structural connectome was constructed and made publicly available by Yeh and colleagues in the following way[31]. Multishell diffusion MRI was acquired using b-values of 1000, 2000, 3000 s/mm^2, each with 90 directions and 1.25 mm iso-voxel resolution Following previous work[5,68], we used the QSDR algorithm[69] implemented in DSI Studio (http://dsi-studio.labsolver.org) to coregister the diffusion data to MNI space, using previously adopted parameters[68]. Deterministic tractography with DSI Studio's modified FACT algorithm[70] then generated 1,000,000 streamlines, using the same parameters as in prior work[5,39,65], specifically, angular cutoff of 55◦, step size of 1.0 mm, minimum length of 10 mm, maximum length of 400mm, spin density function smoothing of 0.0, and a QA threshold determined by DWI signal in the CSF. Each of the streamlines generated was screened for its termination location using an automatically generated white matter mask, to eliminate streamlines with premature termination in the white matter. Entries in the structural connectome A_{ij} were constructed by counting the number of streamlines connecting every pair of regions *i* and *j* in the Lausanne-463[66] and augmented Schaefer-232 atlas[71,72]as done previously[5,68].

5-HT receptor mapping

Details for obtaining the serotonin receptor density distribution have been previously described[46], however we provide a brief summary here. PET data for 210 participants were acquired on a Siemens HRRT scanner operating in 3D acquisition mode with an approximate in-plane resolution of 2mm (1.4 mm in the center of the field of view and 2.4 mm in cortex)[73]. Scan time and frame length were designed according to the radiotracer characteristics. For details on MRI acquisition parameters, which were used to coregister the data to a common atlas, see Knudsen et al[71]. For details on MRI and PET data processing, see the original reference[47].

Extraction of brainstates

Following Cornblath et al.[29], all subjects' fMRI time series for both conditions were concatenated in time and *k*-means clustering was applied to identify clusters of brain activation patterns, or states. Pearson correlation was used as the distance metric and clustering was repeated 50 times with different random initializations before choosing the solution with the best separation of the data. To further assess the stability of clustering and ensure our partitions were reliable, we independently repeated this process 10 times and compared the adjusted mutual information (AMI)[75] between each of the 10 resulting partitions. The partition which shared the greatest total AMI with all other partitions was selected for further analysis. In general, we found that the mutual information shared between partitions was quite high, suggesting consistent clustering across independent runs (*see SI: Assessing the stability of clustering*). We chose the number of clusters *k* via the elbow criterion, i.e. by plotting the variance explained by clustering for *k*=2 through 14 and identifying the "elbow" of the plot, which was between 4-6 across the various partitions. In addition, increasing *k* beyond *k*=5 resulted in a gain of less than 1% of variance explained by clustering, a threshold used previously for determining *k* (*see SI: Choosing k*)[29]. We chose *k*=4 for its straightforward and symmetric interpretation, however the main findings are replicated with *k*=5 in the Supplemental Information.

Characterization of brain states and their hierarchy

Each cluster centroid was characterized by the cosine similarity between it and binary representations of seven a priori defined RSNs[29,37] as shown in the radial plots of Figure 2. Because the mean signal from each scan's regional time series was removed during bandpass filtering, positive values in the centroid reflect activation above the mean (high-amplitude) and negative values reflect activation below the mean (low-amplitude). To quantify the hierarchical relationship between centroids observed in the radial plots, we calculated the Pearson correlation values between all centroids (SI Figure 2) and grouped the anti-correlated pairs together, and refer to each individual centroid as a sub-state and the pair collectively as a meta-state[29,34].

We can extract 1) group-average centroids by taking the mean of all TR's assigned to each cluster (all subjects, all conditions), 2) condition-average centroids by taking the mean of all TR's assigned to each cluster separately for each condition, and 3) individual condition-specific centroids by taking the mean of all TRs assigned to each cluster for a single subject and condition. When taking condition-average centroids (LSD and PL), we find that these two sets of centroids are highly correlated with one another (SI Figure 4d), and thus are also very similar to the group-average centroids shown here. The differences that do exist (quantified here in terms of condition-average differences in cosine-similarity to

RSNs) are consistent with prior observations and a break-down of the brain's functional hierarchy[2,38] (SI Figure 4c)

Temporal brain state dynamics

We then analyzed the temporal dynamics of these brain-states to observe how they change after administration of LSD[29]. The fractional occupancy of each state was determined by the number of TRs assigned to each cluster divided by the total number of TRs. Dwell time was calculated by averaging the length of time spent in a cluster once transitioning to it. Appearance rate was calculated as the total number of times a state was transitioned into per minute. Transition probability values were obtained by calculating the probability that any given state *i* was followed by state *j*.

Energy Calculations

Network control theory allows us to probe the constraints of white-matter connectivity on dynamic brain activity, and to calculate the minimum energy required for the brain to transition from one activation pattern to another[29,39,76]. Here, we utilized network control theory to understand the structural and energetic relationships between these states and the 5-HT2a receptor distribution. While this procedure has been detailed elsewhere[29], we summarize briefly here and in the Supplemental Information. We obtained a representative NxN structural connectome *A* obtained as described above using deterministic tractography from HCP subjects (*see Methods and Materials; Structural Connectivity Network Construction*), where N is the number of regions in our atlas. We then employ a linear time-invariant model:

$$\dot{x}(t) = Ax(t) + Bu(t)$$

where x is a vector of length N containing the regional activity at time *t*. *B* is an NxN matrix that contains the control input weights. *B* is the identity matrix for uniform inputs and contains the regional receptor density information in the diagonal when incorporating the 5-HT receptor maps. For the latter case, the diagonal of *B* was set to 1 plus the normalized regional receptor density value, resulting in a diagonal matrix whose non-zero entries were between 1 and 2. This computational approach allows us to compute the transition energy as the minimum energy required to transition between all pairs of the substates.

The energy calculations in Figure 4a (ii) consisted of separate calculations for each individual's LSD and placebo centroids separately, (iii) utilized each individual's placebo centroids while varying the control input weights *B*, and (iv) used the group average placebo centroids, and *B* was varied for each random permutation. Figure 4b again used each individual's placebo centroids, while varying control input weights *B*.

Lempel-Ziv Complexity

In order to quantify the entropy of each subject's brain-state time series, we chose the widely used Lempel-Ziv algorithm[77,78]; this algorithm assesses the complexity of a binary sequence in terms of the number of unique patterns it contains. A sequence that contains a larger number of unique patterns is more diverse, making it less predictable and therefore more entropic. The normalised Lempel-Ziv complexity (also known as Lempel-Ziv compressibility) is then the number of patterns found in the sequence, divided by the total length of the sequence. In order to apply this algorithm to our brain-state

time series, we first had to convert them to binary sequences that returned 0 or 1 for each time point. To do so, we considered the natural grouping of our 4 brain-states into two meta-states (Meta-State 1 and Meta-State 2). We consider this simplification to be justified by the fact that direct transitions between sub-states (e.g. SOM- to SOM+) were extremely rare (SI Figure 5a), thereby allowing us to reduce the 4-state time series to a 2-state time series while losing very little information regarding transitions.

Statistical Comparisons

The 5-HT_{2a} - weighted inputs from the true receptor distribution were compared to the randomly shuffled distributions via a permutation test where the true receptor distribution was randomly reshuffled and the energy matrix re-calculated 10,000 times. P-values were calculated as the fraction of times that the randomized distribution resulted in a lower energy than the true distribution. All other metric comparisons were achieved using a paired t-test of group means and were corrected for multiple comparisons with Benjamini-Hochberg where correction is indicated.

Code and Data availability

This project used open-source code cited in the main text, as well as code published by Cornblath et al[29]. The data are freely available at https://openneuro.org/datasets/ds003059/versions/1.0.0.

Ethics and Approval

The original study[32] was approved by the National Research Ethics Service committee London-West London and was conducted in accordance with the revised declaration of Helsinki (2000), the International Committee on Harmonization Good Clinical Practice guidelines, and National Health Service Research Governance Framework. Imperial College London sponsored the research, which was conducted under a Home Office license for research with schedule 1 drugs.

Citation and Gender Diversity Statement

Recent work in neuroscience and other fields has identified a bias in citation practices such that papers from women and other minorities are under−cited relative to the number of such papers in the field[79–83]. Here, we sought to proactively consider choosing references that reflect the diversity of the field in thought, form of contribution, gender, and other factors. We used classification of gender based on the first names of the first and last authors[80,84], with possible combinations including male/male, male/female, female/male, and female/female. Excluding self−citations to the first and last authors of our current paper, the references contain 58.67% male/male, 16.00% male/female, 17.33% female/male, and 8.00% female/female. We look forward to future work that could help us to better understand how to support equitable practices in science.

Acknowledgements:

SPS is supported by the National Science Foundation Graduate Research Fellowship (Grant No. DGE-1650441). AIL is supported by the Gates Cambridge Trust. RLC-H is supported by the Alex Mosley Charitable Trust and supporters of the Centre for Psychedelic Research: https://www.imperial.ac.uk/psychedelic-research-centre. The original study received support from a Crowd Funding Campaign and the Beckley Foundation, as part of the Beckley-Imperial Research Programme. JC is supported by the Spanish Ministry of Science and Innovation under the fellowship

BES-2017-080364. GD is supported by the Spanish Research Project (ref. PID2019-105772GB-I00 AEI FEDER EU), funded by the Spanish Ministry of Science, Innovation and Universities (MCIU), State Research Agency (AEI) and European Regional Development Funds (FEDER); HBP SGA3 Human Brain Project Specific Grant Agreement 3 (Grant Agreement No. 945539), funded by the EU H2020 FET Flagship program and SGR Research Support Group support (ref. 2017 SGR 1545), funded by the Catalan Agency for Management of University and Research Grants (AGAUR). MLK is supported by the Center for Music in the Brain, funded by the Danish National Research Foundation (DNRF117), and Centre for Eudaimonia and Human Flourishing funded by the Pettit and Carlsberg Foundations. EAS is supported by the Stephen Erskine Fellowship from Queens' College, Cambridge. AK is supported by the National Institutes of Health (RF1MH123232, R01NS102646 and R21NS104634).

References:

1. Shulgin AT, Shulgin A. *Tihkal: The Continuation*. Transform Press; 1997.
2. Carhart-Harris RL, Friston KJ. REBUS and the Anarchic Brain: Toward a Unified Model of the Brain Action of Psychedelics. Barker EL, ed. *Pharmacol Rev*. 2019;71(3):316-344. doi:10.1124/pr.118.017160
3. Carhart-Harris RL, Leech R, Hellyer PJ, et al. The entropic brain: a theory of conscious states informed by neuroimaging research with psychedelic drugs. *Front Hum Neurosci*. 2014;8. doi:10.3389/fnhum.2014.00020
4. Friston K. The free-energy principle: a unified brain theory? *Nat Rev Neurosci*. 2010;11(2):127-138. doi:10.1038/nrn2787
5. Luppi AI, Carhart-Harris RL, Roseman L, Pappas I, Menon DK, Stamatakis EA. LSD alters dynamic integration and segregation in the human brain. *NeuroImage*. 2021;227:117653. doi:10.1016/j.neuroimage.2020.117653
6. Deco G, Cruzat J, Cabral J, et al. Whole-Brain Multimodal Neuroimaging Model Using Serotonin Receptor Maps Explains Non-linear Functional Effects of LSD. *Curr Biol*. 2018;28(19):3065-3074.e6. doi:10.1016/j.cub.2018.07.083
7. Kringelbach ML, Cruzat J, Cabral J, et al. Dynamic coupling of whole-brain neuronal and neurotransmitter systems. *Proc Natl Acad Sci*. 2020;117(17):9566-9576. doi:10.1073/pnas.1921475117
8. Herzog R, Mediano PAM, Rosas FE, et al. A mechanistic model of the neural entropy increase elicited by psychedelic drugs. *Sci Rep*. 2020;10(1):17725. doi:10.1038/s41598-020-74060-6
9. Lurie D, Kessler D, Bassett D, et al. On the nature of time-varying functional connectivity in resting fMRI. Published online December 24, 2018. doi:10.31234/osf.io/xtzre
10. Preti MG, Bolton TA, Van De Ville D. The dynamic functional connectome: State-of-the-art and perspectives. *NeuroImage*. 2017;160:41-54. doi:10.1016/j.neuroimage.2016.12.061
11. Vohryzek J, Deco G, Cessac B, Kringelbach ML, Cabral J. Ghost Attractors in Spontaneous Brain Activity: Recurrent Excursions Into Functionally-Relevant BOLD Phase-Locking States. *Front Syst Neurosci*. 2020;14. doi:10.3389/fnsys.2020.00020
12. Cabral J, Kringelbach ML, Deco G. Exploring the network dynamics underlying brain activity during rest. *Prog Neurobiol*. 2014;114:102-131. doi:10.1016/j.pneurobio.2013.12.005
13. Cabral J, Kringelbach ML, Deco G. Functional connectivity dynamically evolves on multiple time-scales over a static structural connectome: Models and mechanisms. *NeuroImage*. 2017;160:84-96. doi:10.1016/j.neuroimage.2017.03.045
14. Deco G, Kringelbach ML. Great Expectations: Using Whole-Brain Computational Connectomics for Understanding Neuropsychiatric Disorders. *Neuron*. 2014;84(5):892-905. doi:10.1016/j.neuron.2014.08.034

15. Kringelbach ML, Deco G. Brain States and Transitions: Insights from Computational Neuroscience. *Cell Rep*. 2020;32(10):108128. doi:10.1016/j.celrep.2020.108128
16. Hutchison RM, Womelsdorf T, Allen EA, et al. Dynamic functional connectivity: promise, issues, and interpretations. *NeuroImage*. 2013;80:360-378. doi:10.1016/j.neuroimage.2013.05.079
17. Shine JM, Bissett PG, Bell PT, et al. The Dynamics of Functional Brain Networks: Integrated Network States during Cognitive Task Performance. *Neuron*. 2016;92(2):544-554. doi:10.1016/j.neuron.2016.09.018
18. Esfahlani FZ, Jo Y, Faskowitz J, et al. High-amplitude cofluctuations in cortical activity drive functional connectivity. *Proc Natl Acad Sci*. 2020;117(45):28393-28401. doi:10.1073/pnas.2005531117
19. Cabral J, Vidaurre D, Marques P, et al. Cognitive performance in healthy older adults relates to spontaneous switching between states of functional connectivity during rest. *Sci Rep*. 2017;7(1):5135. doi:10.1038/s41598-017-05425-7
20. Alonso Martínez S, Deco G, Ter Horst GJ, Cabral J. The Dynamics of Functional Brain Networks Associated With Depressive Symptoms in a Nonclinical Sample. *Front Neural Circuits*. 2020;14. doi:10.3389/fncir.2020.570583
21. Demertzi A, Tagliazucchi E, Dehaene S, et al. Human consciousness is supported by dynamic complex patterns of brain signal coordination. *Sci Adv*. 2019;5(2):eaat7603. doi:10.1126/sciadv.aat7603
22. Luppi AI, Craig MM, Pappas I, et al. Consciousness-specific dynamic interactions of brain integration and functional diversity. *Nat Commun*. 2019;10(1):4616. doi:10.1038/s41467-019-12658-9
23. Luppi AI, Mediano PAM, Rosas FE, et al. Paths to Oblivion: Common Neural Mechanisms of Anaesthesia and Disorders of Consciousness. *bioRxiv*. Published online February 16, 2021:2021.02.14.431140. doi:10.1101/2021.02.14.431140
24. Barttfeld P, Uhrig L, Sitt JD, Sigman M, Jarraya B, Dehaene S. Signature of consciousness in the dynamics of resting-state brain activity. *Proc Natl Acad Sci*. 2015;112(3):887-892. doi:10.1073/pnas.1418031112
25. Huang Z, Zhang J, Wu J, Mashour GA, Hudetz AG. Temporal circuit of macroscale dynamic brain activity supports human consciousness. *Sci Adv*. 2020;6(11):eaaz0087. doi:10.1126/sciadv.aaz0087
26. Luppi AI, Golkowski D, Ranft A, et al. Brain network integration dynamics are associated with loss and recovery of consciousness induced by sevoflurane. *Hum Brain Mapp*. n/a(n/a). doi:https://doi.org/10.1002/hbm.25405
27. Hutchison RM, Hutchison M, Manning KY, Menon RS, Everling S. Isoflurane induces dose-dependent alterations in the cortical connectivity profiles and dynamic properties of the brain's functional architecture. *Hum Brain Mapp*. 2014;35(12):5754-5775. doi:https://doi.org/10.1002/hbm.22583
28. Lord L-D, Expert P, Atasoy S, et al. Dynamical exploration of the repertoire of brain networks at rest is modulated by psilocybin. *NeuroImage*. 2019;199:127-142. doi:10.1016/j.neuroimage.2019.05.060
29. Cornblath EJ, Ashourvan A, Kim JZ, et al. Temporal sequences of brain activity at rest are constrained by white matter structure and modulated by cognitive demands. *Commun Biol*. 2020;3(1):261. doi:10.1038/s42003-020-0961-x
30. Braun U, Harneit A, Pergola G, et al. Brain state stability during working memory is explained by network control theory, modulated by dopamine D1/D2 receptor function, and diminished in schizophrenia. *bioRxiv*. Published online June 23, 2019:679670. doi:10.1101/679670
31. Yeh F-C, Panesar S, Fernandes D, et al. Population-averaged atlas of the macroscale human structural connectome and its network topology. *NeuroImage*. 2018;178:57-68. doi:10.1016/j.neuroimage.2018.05.027
32. Carhart-Harris RL, Muthukumaraswamy S, Roseman L, et al. Neural correlates of the LSD

experience revealed by multimodal neuroimaging. *Proc Natl Acad Sci*. 2016;113(17):4853-4858. doi:10.1073/pnas.1518377113
33. Allen EA, Damaraju E, Plis SM, Erhardt EB, Eichele T, Calhoun VD. Tracking Whole-Brain Connectivity Dynamics in the Resting State. *Cereb Cortex*. 2014;24(3):663-676. doi:10.1093/cercor/bhs352
34. Gutierrez-Barragan D, Basson MA, Panzeri S, Gozzi A. Infraslow State Fluctuations Govern Spontaneous fMRI Network Dynamics. *Curr Biol*. 2019;29(14):2295-2306.e5. doi:10.1016/j.cub.2019.06.017
35. Vidaurre D, Smith SM, Woolrich MW. Brain network dynamics are hierarchically organized in time. *Proc Natl Acad Sci*. 2017;114(48):12827-12832. doi:10.1073/pnas.1705120114
36. Chen RH, Ito T, Kulkarni KR, Cole MW. The Human Brain Traverses a Common Activation-Pattern State Space Across Task and Rest. *Brain Connect*. 2018;8(7):429-443. doi:10.1089/brain.2018.0586
37. Thomas Yeo BT, Krienen FM, Sepulcre J, et al. The organization of the human cerebral cortex estimated by intrinsic functional connectivity. *J Neurophysiol*. 2011;106(3):1125-1165. doi:10.1152/jn.00338.2011
38. Girn M, Roseman L, Bernhardt B, Smallwood J, Carhart-Harris R, Spreng RN. Serotonergic psychedelic drugs LSD and psilocybin reduce the hierarchical differentiation of unimodal and transmodal cortex. *bioRxiv*. Published online April 14, 2021:2020.05.01.072314. doi:10.1101/2020.05.01.072314
39. Gu S, Pasqualetti F, Cieslak M, et al. Controllability of structural brain networks. *Nat Commun*. 2015;6(1):8414. doi:10.1038/ncomms9414
40. Betzel RF, Gu S, Medaglia JD, Pasqualetti F, Bassett DS. Optimally controlling the human connectome: the role of network topology. *Sci Rep*. 2016;6(1):30770. doi:10.1038/srep30770
41. Karrer TM, Kim JZ, Stiso J, et al. A practical guide to methodological considerations in the controllability of structural brain networks. *J Neural Eng*. 2020;17(2):026031. doi:10.1088/1741-2552/ab6e8b
42. Kraehenmann R, Pokorny D, Aicher H, et al. LSD Increases Primary Process Thinking via Serotonin 2A Receptor Activation. *Front Pharmacol*. 2017;8. doi:10.3389/fphar.2017.00814
43. Kraehenmann R, Pokorny D, Vollenweider L, et al. Dreamlike effects of LSD on waking imagery in humans depend on serotonin 2A receptor activation. *Psychopharmacology (Berl)*. 2017;234(13):2031-2046. doi:10.1007/s00213-017-4610-0
44. Preller KH, Burt JB, Ji JL, et al. Changes in global and thalamic brain connectivity in LSD-induced altered states of consciousness are attributable to the 5-HT2A receptor. Hunt LT, Behrens TE, eds. *eLife*. 2018;7:e35082. doi:10.7554/eLife.35082
45. Preller KH, Schilbach L, Pokorny T, Flemming J, Seifritz E, Vollenweider FX. Role of the 5-HT2A Receptor in Self- and Other-Initiated Social Interaction in Lysergic Acid Diethylamide-Induced States: A Pharmacological fMRI Study. *J Neurosci*. 2018;38(14):3603-3611. doi:10.1523/JNEUROSCI.1939-17.2018
46. Duerler P, Schilbach L, Stämpfli P, Vollenweider FX, Preller KH. LSD-induced increases in social adaptation to opinions similar to one's own are associated with stimulation of serotonin receptors. *Sci Rep*. 2020;10(1):12181. doi:10.1038/s41598-020-68899-y
47. Beliveau V, Ganz M, Feng L, et al. A High-Resolution *In Vivo* Atlas of the Human Brain's Serotonin System. *J Neurosci*. 2017;37(1):120-128. doi:10.1523/JNEUROSCI.2830-16.2016
48. Carhart-Harris RL. The entropic brain - revisited. *Neuropharmacology*. 2018;142:167-178. doi:10.1016/j.neuropharm.2018.03.010
49. Schartner MM, Carhart-Harris RL, Barrett AB, Seth AK, Muthukumaraswamy SD. Increased spontaneous MEG signal diversity for psychoactive doses of ketamine, LSD and psilocybin. *Sci Rep*. 2017;7(1):46421. doi:10.1038/srep46421
50. Timmermann C, Roseman L, Schartner M, et al. Neural correlates of the DMT experience assessed with multivariate EEG. *Sci Rep*. 2019;9(1):16324. doi:10.1038/s41598-019-51974-4

51. Lebedev AV, Kaelen M, Lövdén M, et al. LSD-induced entropic brain activity predicts subsequent personality change: LSD-Induced Entropic Brain Activity. *Hum Brain Mapp*. 2016;37(9):3203-3213. doi:10.1002/hbm.23234
52. Varley TF, Carhart-Harris R, Roseman L, Menon DK, Stamatakis EA. Serotonergic psychedelics LSD & psilocybin increase the fractal dimension of cortical brain activity in spatial and temporal domains. *NeuroImage*. 2020;220:117049. doi:10.1016/j.neuroimage.2020.117049
53. Raichle ME, MacLeod AM, Snyder AZ, Powers WJ, Gusnard DA, Shulman GL. A default mode of brain function. *Proc Natl Acad Sci*. 2001;98(2):676-682. doi:10.1073/pnas.98.2.676
54. Raichle ME. The Brain's Default Mode Network. *Annu Rev Neurosci*. 2015;38(1):433-447. doi:10.1146/annurev-neuro-071013-014030
55. Buckner RL, DiNicola LM. The brain's default network: updated anatomy, physiology and evolving insights. *Nat Rev Neurosci*. 2019;20(10):593-608. doi:10.1038/s41583-019-0212-7
56. Yeshurun Y, Nguyen M, Hasson U. The default mode network: where the idiosyncratic self meets the shared social world. *Nat Rev Neurosci*. 2021;22(3):181-192. doi:10.1038/s41583-020-00420-w
57. Northoff G, Wainio-Theberge S, Evers K. Is temporo-spatial dynamics the "common currency" of brain and mind? In Quest of "Spatiotemporal Neuroscience." *Phys Life Rev*. 2020;33:34-54. doi:10.1016/j.plrev.2019.05.002
58. Atasoy S, Roseman L, Kaelen M, Kringelbach ML, Deco G, Carhart-Harris RL. Connectome-harmonic decomposition of human brain activity reveals dynamical repertoire re-organization under LSD. *Sci Rep*. 2017;7(1):17661. doi:10.1038/s41598-017-17546-0
59. Luppi AI, Vohryzek J, Kringelbach ML, et al. Connectome Harmonic Decomposition of Human Brain Dynamics Reveals a Landscape of Consciousness. *bioRxiv*. Published online August 10, 2020:2020.08.10.244459. doi:10.1101/2020.08.10.244459
60. Mediano PAM, Rosas FE, Timmermann C, et al. Effects of external stimulation on psychedelic state neurodynamics. *bioRxiv*. Published online November 2, 2020:2020.11.01.356071. doi:10.1101/2020.11.01.356071
61. Atasoy S, Vohryzek J, Deco G, Carhart-Harris RL, Kringelbach ML. Chapter 4 - Common neural signatures of psychedelics: Frequency-specific energy changes and repertoire expansion revealed using connectome-harmonic decomposition. In: Calvey T, ed. *Progress in Brain Research*. Vol 242. Psychedelic Neuroscience. Elsevier; 2018:97-120. doi:10.1016/bs.pbr.2018.08.009
62. Dittrich A. The Standardized Psychometric Assessment of Altered States of Consciousness (ASCs) in Humans. *Pharmacopsychiatry*. 1998;31(S 2):80-84.
63. Studerus E, Gamma A, Vollenweider FX. Psychometric Evaluation of the Altered States of Consciousness Rating Scale (OAV). *PLOS ONE*. 2010;5(8):e12412. doi:10.1371/journal.pone.0012412
64. Nozari E, Stiso J, Caciagli L, et al. Is the brain macroscopically linear? A system identification of resting state dynamics. *ArXiv201212351 Cs Eess Math Q-Bio*. Published online December 22, 2020. Accessed April 28, 2021. http://arxiv.org/abs/2012.12351
65. Schulz M-A, Yeo BTT, Vogelstein JT, et al. Different scaling of linear models and deep learning in UKBiobank brain images versus machine-learning datasets. *Nat Commun*. 2020;11(1):4238. doi:10.1038/s41467-020-18037-z
66. Cammoun L, Gigandet X, Meskaldji D, et al. Mapping the human connectome at multiple scales with diffusion spectrum MRI. *J Neurosci Methods*. 2012;203(2):386-397. doi:10.1016/j.jneumeth.2011.09.031
67. Van Essen DC, Smith SM, Barch DM, Behrens TEJ, Yacoub E, Ugurbil K. The WU-Minn Human Connectome Project: An overview. *NeuroImage*. 2013;80:62-79. doi:10.1016/j.neuroimage.2013.05.041
68. Luppi AI, Stamatakis EA. Combining network topology and information theory to construct representative brain networks. *Netw Neurosci*. 2021;5(1):96-124. doi:10.1162/netn_a_00170
69. Yeh F-C, Wedeen VJ, Tseng W-YI. Estimation of fiber orientation and spin density distribution by diffusion deconvolution. *NeuroImage*. 2011;55(3):1054-1062.

doi:10.1016/j.neuroimage.2010.11.087
70. Yeh F-C, Verstynen TD, Wang Y, Fernández-Miranda JC, Tseng W-YI. Deterministic Diffusion Fiber Tracking Improved by Quantitative Anisotropy. *PLOS ONE*. 2013;8(11):e80713. doi:10.1371/journal.pone.0080713
71. Schaefer A, Kong R, Gordon EM, et al. Local-Global Parcellation of the Human Cerebral Cortex from Intrinsic Functional Connectivity MRI. *Cereb Cortex*. 2018;28(9):3095-3114. doi:10.1093/cercor/bhx179
72. Tian Y, Margulies DS, Breakspear M, Zalesky A. Topographic organization of the human subcortex unveiled with functional connectivity gradients. *Nat Neurosci*. 2020;23(11):1421-1432. doi:10.1038/s41593-020-00711-6
73. Olesen OV, Sibomana M, Keller SH, et al. Spatial resolution of the HRRT PET scanner using 3D-OSEM PSF reconstruction. In: *2009 IEEE Nuclear Science Symposium Conference Record (NSS/MIC)*. ; 2009:3789-3790. doi:10.1109/NSSMIC.2009.5401892
74. Knudsen GM, Jensen PS, Erritzoe D, et al. The Center for Integrated Molecular Brain Imaging (Cimbi) database. *NeuroImage*. 2016;124:1213-1219. doi:10.1016/j.neuroimage.2015.04.025
75. Nguyen XV. The Adjusted Mutual Information. Accessed April 16, 2021. https://www.mathworks.com/matlabcentral/fileexchange/33144-the-adjusted-mutual-information
76. Tang E, Giusti C, Baum GL, et al. Developmental increases in white matter network controllability support a growing diversity of brain dynamics. *Nat Commun*. 2017;8(1):1252. doi:10.1038/s41467-017-01254-4
77. Lempel A, Ziv J. On the Complexity of Finite Sequences. *IEEE Trans Inf Theory*. 1976;22(1):75-81. doi:10.1109/TIT.1976.1055501
78. Thai Q. calc_lz_complexity. Accessed May 5, 2021. https://www.mathworks.com/matlabcentral/fileexchange/38211-calc_lz_complexity
79. Maliniak D, Powers R, Walter BF. The Gender Citation Gap in International Relations. *Int Organ*. 2013;67(4):889-922. doi:10.1017/S0020818313000209
80. Dworkin JD, Linn KA, Teich EG, Zurn P, Shinohara RT, Bassett DS. The extent and drivers of gender imbalance in neuroscience reference lists. *Nat Neurosci*. 2020;23(8):918-926. doi:10.1038/s41593-020-0658-y
81. Dion ML, Sumner JL, Mitchell SM. Gendered Citation Patterns across Political Science and Social Science Methodology Fields. *Polit Anal*. 2018;26(3):312-327. doi:10.1017/pan.2018.12
82. Chakravartty P, Kuo R, Grubbs V, McIlwain C. #CommunicationSoWhite. *J Commun*. 2018;68(2):254-266. doi:10.1093/joc/jqy003
83. Caplar N, Tacchella S, Birrer S. Quantitative evaluation of gender bias in astronomical publications from citation counts. *Nat Astron*. 2017;1(6):1-5. doi:10.1038/s41550-017-0141
84. Dale Zhou, Jennifer Stiso, Eli Cornblath, et al. *Dalejn/CleanBib: V1.1.1*. Zenodo; 2020. doi:10.5281/zenodo.4104748